1968, *Bull. Astr. Inst. Netherlands* **19** 363–373;
Communication from the Netherlands Foundation for Radio Astronomy and the Observatory at Leiden

A NEUTRAL-HYDROGEN FEATURE AT $l^{II} = -11°$, $b^{II} = +3°$

P. CUGNON*

Received 11 October 1967

This paper describes a hydrogen feature at $l^{II} = -11°$, $b^{II} = +3°$ with an abnormal radial velocity of +50 km/sec and a velocity dispersion of about 10 km/sec. Only part (about 30 square degrees) of the whole object can be observed from the Netherlands. Five interpretations are considered: 1) part of the shell of a supernova, or of a "superexplosion", 2) an extragalactic object, 3) a structural feature located near the galactic centre, 4) a high-velocity cloud, and 5) a distant spiral arm of the Galaxy.

1. Observations

A small number of the 21-cm profiles from the Kootwijk survey (MULLER and WESTERHOUT, 1957) shows an unexpected secondary peak at radial velocity +50 km/sec. The positions of these profiles are

l^I	b^I
314°.3	+4°.7
316.2	+2.4
316.9	+4.1
318.2	+2.5

In order to obtain a better picture of this feature, a new set of observations was made at Dwingeloo with the 25-m radio telescope. The receiver has been described by MULLER *et al.* (1966).

The measurements extend between radial velocities −50 and +150 km/sec with respect to the local standard of rest. The positions which were observed are shown in figure 1. The bandwidth used was 16 kHz. Four independent measurements were made at each point, in December 1965 and January 1966. The reduction was performed in the usual way (RAIMOND, 1966; MULLER *et al.*, 1966) except for a revised zero-correction as a function of the altitude, which becomes very important close to the horizon. The average of the four profiles obtained at each position was used in the further investigations. The averaged profiles are shown in figure 2 (at the end of the paper).

* Aspirant au Fonds National Belge de la Recherche Scientifique. Present address: Institut d'Astrophysique, Cointe-Sclessin, Belgium.

2. Description of the results

Isophote charts with respect to one of the galactic coordinates and the radial velocity are shown in figure 3. The feature at +50 km/sec appears well separated from the main galactic structure. Isophote charts with respect to both galactic coordinates and for several radial velocities are shown in figure 4. In this figure another feature appears at +15 and +25 km/sec that seems to follow a line arising from the galactic plane at $l^{II} = -3°$ extending up to $l^{II} = -10°$ and $b^{II} = +8°$ and perhaps coming down again farther from the centre, so that the 50-km/sec feature is located in a region where a deficiency in neutral hydrogen for lower velocities is observed. On the other hand, by plotting on a graph in l^{II}, b^{II} the isolated maximum intensities for a

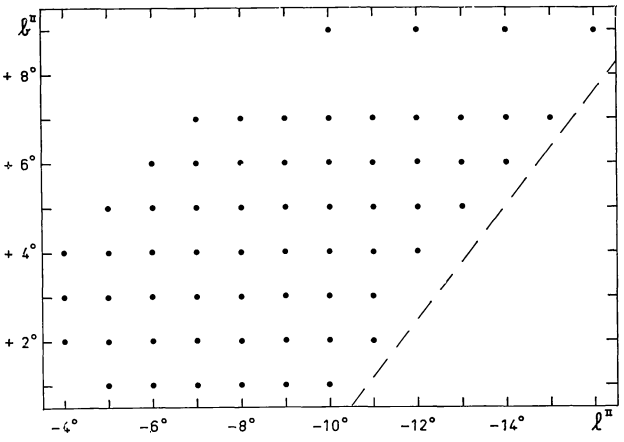

Figure 1. The grid of the observed points; the dashed line is approximately the southern limit of observation.

few velocities, one can observe a certain regularity in the distribution of the points along a smooth curve (figure 6). In section 4.3 I shall make a few further remarks about the possible significance of this distribution.

3. The feature at 50 km/sec

It was not difficult to subtract the galactic structure from the 50-km/sec peak when the separation between it and the main peak was well defined, i.e., at galactic latitudes higher than $+2°$. The following procedure was used. A Gaussian curve was fitted to that part of the 50-km/sec peak which could be considered as nearly free from influence of the galactic background. The component found was subtracted from the whole profile and the result smoothed. In order to avoid large discordances between nearby profiles, I plotted the intensities of the resulting profiles as a function of the galactic longitude for a number of radial velocities at each latitude. Smooth curves passing through the points were drawn and used to adjust the profiles, if necessary. The 50-km/sec peak was finally obtained by subtracting these adjusted profiles from the original ones.

The separation was much more difficult at lower latitudes, because of the superposition of several components in the 0 to $+50$-km/sec range. In order to obtain at least a rough estimate of the 50-km/sec contribution, I extrapolated by hand the main peak; the subtraction of this model from the original profile gave a superposition of two apparent components, one centred at about 30 km/sec in addition to the 50-km/sec peak. They were separated by assuming Gaussian shapes for both. It is easy to see that any error in the extrapolation of the galactic structure would strongly influence the final result.

Table 1 gives a summary of the characteristics of the profiles with the galactic contribution and the $+30$-km/sec feature removed as explained above. It contains:
Columns 1 and 2: Galactic longitude and latitude.
Column 3: Number of hydrogen atoms per cm^2 integrated along the line of sight, given by

$$N_H = 1.822 \times 10^{18} \int T_b \, dV$$

for small T_b. As usual, the integral is replaced by a sum,

$$N_H = 1.822 \times 10^{18} \sum_i T_{bi} \Delta V,$$

where T_b is expressed in °K, ΔV being the velocity interval between two points in the profile, 2 km/sec in this case.
Column 4: Mean radial velocity,

$$V = \sum_i T_{bi} V_i / \sum_i T_{bi}.$$

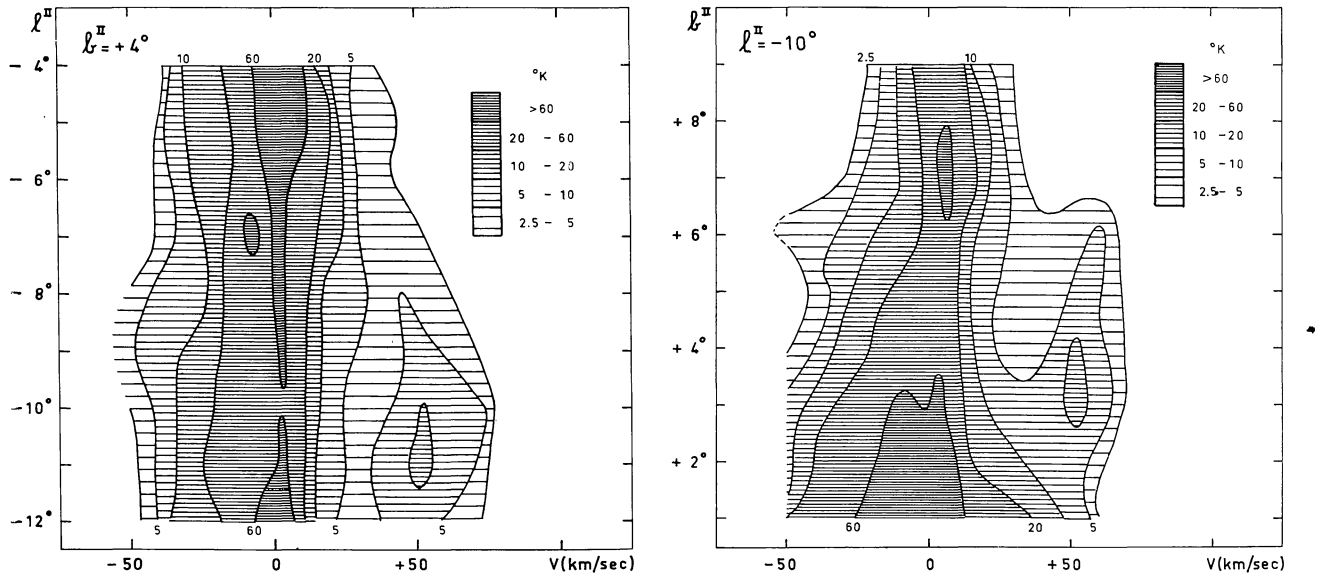

Figure 3. Contour lines of brightness temperature as a function of the radial velocity and, respectively, the galactic longitude at $b^{II} = +4°$ and the galactic latitude at $l^{II} = -10°$.

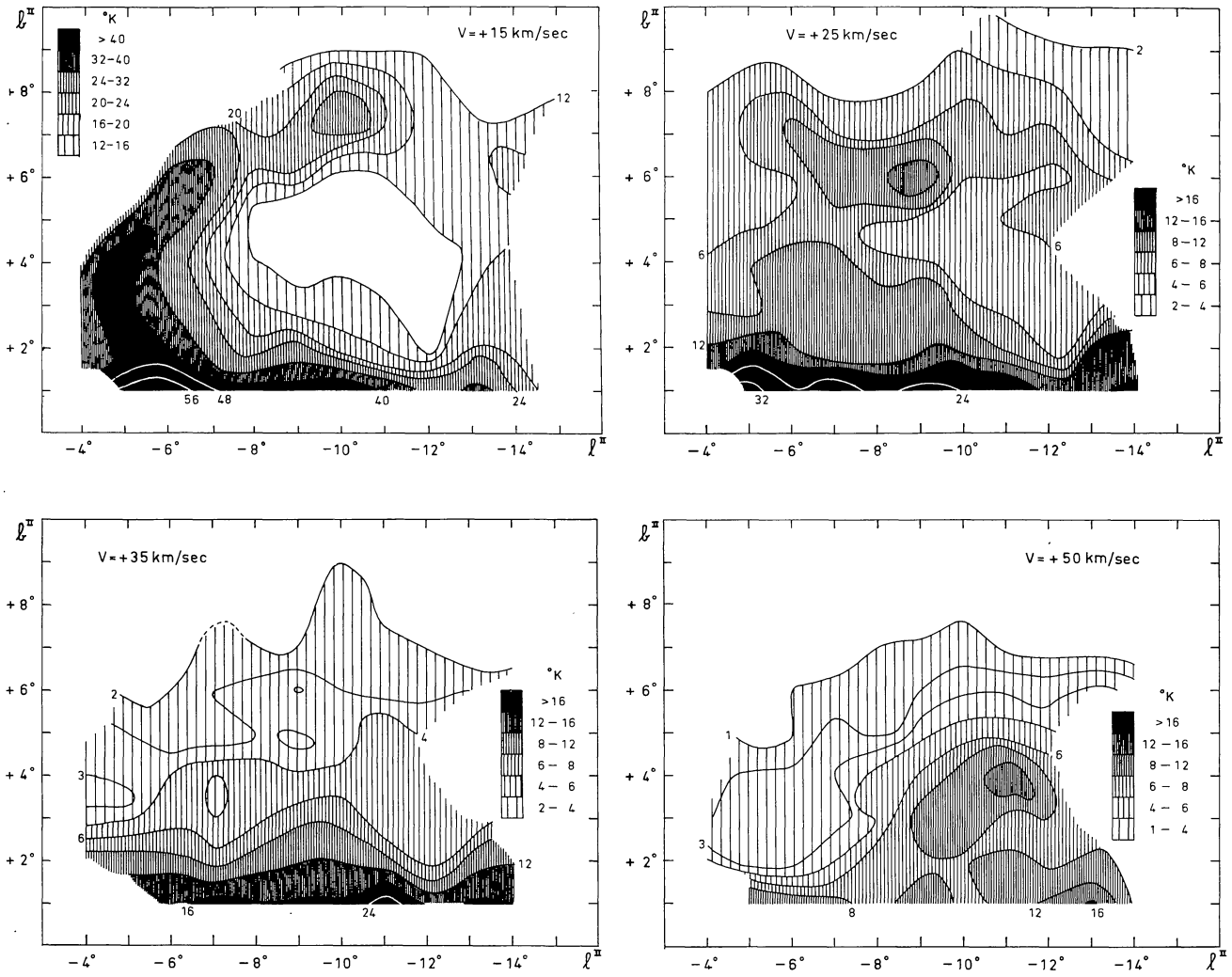

Figure 4. Contour lines of brightness temperature as a function of both galactic coordinates at four different velocities; Kerr's contour diagrams were used to complete these pictures.

Column 5: Velocity dispersion,

$$\sigma = (\sum_i T_{bi} V_i^2 / \sum_i T_{bi} - V^2)^{\frac{1}{2}}.$$

Column 6: Residual velocity, $V_r(l^{II}, b^{II}) = V(l^{II}, b^{II}) - V(-11°, +4°)$; the mean radial velocity at $-11°$, $+4°$ was chosen as a reference velocity because of the narrowness of the peak at this position. The fact that an important part of the feature could not be observed made it impossible to determine a true mean velocity. For this reason the velocity residuals in column 6 should be viewed with caution.

A number of quantities related to the whole feature were also calculated:

$$N' = \sum_{l,b} N_H(l, b) = 81.4 \times 10^{20} \text{ atoms} \cdot \text{cm}^{-2} \cdot \text{sq deg}^{-2},$$

$$\langle \sigma^2 \rangle = \sum_{l,b} N_H(l, b) \sigma^2(l, b) / N' = 107.5 \text{ km}^2 \cdot \text{sec}^{-2},$$

$$\langle V_r^2 \rangle = \sum_{l,b} N_H(l, b) V_r^2(l, b) / N' = 4.2 \text{ km}^2 \cdot \text{sec}^{-2}.$$

Before investigating some hypotheses about the nature of the 50-km/sec cloud, it was helpful to look at contour diagrams of observations made from Australia and kindly put at my disposal before publication by Dr. F. J. Kerr. Though these southern-hemisphere observations are confined to the region between $b^{II} = -2°$

TABLE 1

Properties of the +50-km/sec feature

l^{II}	b^{II}	N_H (10^{20} cm^{-2})	V	σ (km/sec)	V_r	l^{II}	b^{II}	N_H (10^{20} cm^{-2})	V	σ (km/sec)	V_r
−6°	+2°	1.04	54.55	10.59	+3.31	−10°	+1°	2.38	50.77	9.12	−0.57
	+3	1.55	51.86	9.32	+0.62		+2	2.68	50.96	9.58	−0.28
	+4	1.00	50.93	9.50	−0.31		+3	4.58	51.72	8.93	+0.48
	+5	(0.31)	(42.97)		(−9.27)		+4	4.55	51.34	10.05	+0.08
	+6	(0.59)	(55.41)		(+4.17)		+5	2.88	51.50	10.40	+0.26
−7	+1	(1.07)	(58.51)	(7.24)	(+7.27)		+6	(2.11)	(53.35)	(10.77)	(+2.11)
	+2	1.35	51.75	10.65	+0.51		+7	0.58	51.26		+0.02
	+3	1.65	50.46	12.03	−0.78						
	+4	1.53	47.57	9.97	−3.67	−11	+2	4.54	50.56	12.34	−0.68
	+5	0.96	50.67	6.08	−0.57		+3	4.25	52.43	11.18	+1.19
	+6	0.66	53.01		+1.38		+4	4.03	51.24	6.78	0.00
−8	+1	(1.18)	(51.80)	(8.47)	(+0.56)		+5	2.47	52.15	10.43	+0.89
	+2	(1.60)	(55.63)	(6.62)	(+4.39)		+6	1.37	51.63	10.56	+0.39
	+3	2.28	50.55	10.62	−0.89		+7	<0.30			
	+4	2.51	47.12	11.65	−4.12	−12	+4	2.99	49.93	8.38	−1.31
	+5	1.25	44.76	11.87	−6.48		+5	2.87	47.81	13.69	−3.43
	+6	1.38	54.81	11.08	+3.37		+6	1.27	48.66	11.23	−2.58
	+7	0.43	49.96		−1.28		+7	<0.30			
−9	+1	(1.80)	(50.73)	(7.21)	(−0.56)						
	+2	(2.68)	(48.75)	(7.47)	(−2.49)	−13	+5	2.22	50.99	12.99	−0.25
	+3	3.45	51.76	8.63	+0.32		+6	1.79	49.18	11.49	−2.06
	+4	3.07	50.03	11.47	−1.21		+7	<0.30			
	+5	1.78	53.59	8.77	+2.29						
	+6	1.24	55.53	9.69	+4.29	−14	+6	1.19	49.42	7.23	−1.82
	+7	0.52	50.95		−0.29		+7	<0.30			

and $b^{II} = +2°$, it was possible to follow a feature with high velocity (between +40 and +60 km/sec) from $l^{II} = -13°$ to $l^{II} = -19°$ and perhaps further. The possibility that the 50-km/sec cloud is related to this feature will be investigated in section 4.5. However, as there appears to be a break between these two features at $l^{II} = -12°$, and as they will be discussed as separate objects in some of the following analysis, the cloud at $l^{II} = -11°$, $b^{II} = +3°$ has been analysed separately by expressing the distribution of hydrogen within the feature integrated along the line of sight as a bivariate normal distribution. The results of this analysis together with the observed densities are shown in figure 5. The characteristics of this model are: position angle of the major axis = 80, dispersion in the direction of the major axis = 2°.9, dispersion in the direction of the minor axis = 2°.0, central density $N_{Hc} = 4.4 \times 10^{20}$ cm^{-2}, position of the centre $l_c^{II} = -11°$, $b_c^{II} = +3°$.

A comparison between the integrated values of N_H over l^{II} and b^{II} (model) and the value of N' indicates that about half of the cloud is above the southern limit of observation. Furthermore, the observed lines of equal density (full-drawn curves in figure 5) attribute roughly the same position to the centre as does the

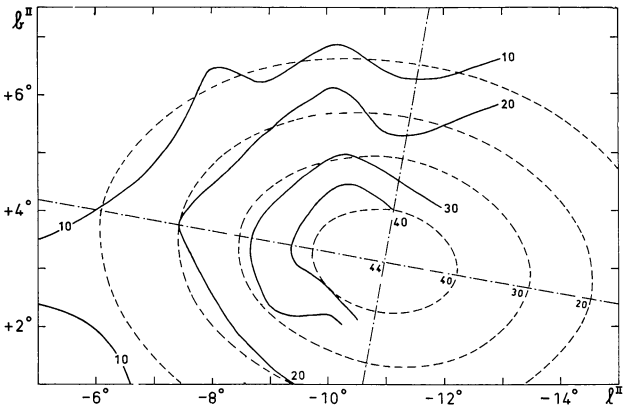

Figure 5. Contour lines of equal hydrogen surface density as integrated along the line of sight, after subtraction of the galactic structure (full-drawn curves). The dashed curves are the corresponding ellipses deduced from the Gaussian model. The unit of surface density is 10^{19} atoms · cm^{-2}.

model. In table 2 the physical properties of the cloud as derived from the model are summarized for a number of possible values of the distance.

TABLE 2

Physical properties of the cloud as a function of distance

r (kpc)	R (kpc)	n_{Hc} (cm^{-3})	D (pc)	M_H ($M_\odot$)	z (kpc)
0.1	9.9	13.27	4.2	4×10^2	0.0054
1.0	9.0	1.33	41.9	4×10^4	0.054
10.0	1.9	0.13	419	4×10^6	0.54
50.0	40.2	0.026	2095	10^8	2.70
200.0	190	0.007	8380	1.6×10^9	10.80

r : Distance from the Sun.
R : Distance from the galactic centre.
n_{Hc}: Number of hydrogen atoms per cm^3 at the centre of the cloud corresponding to the spherically symmetrical Gaussian model described in section 4.
D : Mean dispersion (as defined in section 3).
M_H: Hydrogen mass.
z : Distance from the galactic plane.

4. Interpretations

In the following subsections some possible interpretations will be investigated. They are: 1) a fragment of a supernova shell or of a past "superexplosion", 2) an extragalactic object, 3) a feature located near the galactic centre, 4) a high-velocity cloud, and 5) a distant spiral arm.

In order to limit the range of possibilities, I shall use the same method as PRATA (1964). The scalar virial theorem can be written

$$\tfrac{1}{2}\frac{d^2I}{dt^2} = 2T+3U+W,$$

if one neglects the magnetic terms; Prata has observed that in most cases these terms are too small to play any role if one admits reasonable values for the field. The symbols in the above formula have the following meaning:

T : kinetic energy of mass elements within the cloud,

$3U/2$: thermal energy,

$$U = \int P\,dV,$$

W : gravitational energy,

$$W = \int \boldsymbol{S}.\nabla\boldsymbol{\Phi}\,dm,$$

where $\boldsymbol{S}$ is the position vector in the cloud and $\boldsymbol{\Phi}$ the gravitational potential,

I : moment of inertia with respect to the centre of the cloud,

$$I = \int S^2\,dm.$$

In order to estimate each contribution I have made use of a simplified Gaussian model, i.e.,

$$n_H = n_{Hc} \exp(-S^2/2D^2),$$

where n_H is the number of neutral hydrogen atoms per cm^3, the index c referring to the centre; $D = r(\sin 2°.9 \times \sin 2°.0)^{\frac{1}{2}}$ is the geometrical mean of the linear dispersions in the elliptical model; r is the distance from the Sun, and S is the distance between any point and the centre of the cloud.

Following Prata, the kinetic and thermal energies are combined into a single term, given by

$$2T' = 2T+3U = 2M(\tfrac{3}{2}\langle V_r^2\rangle+\tfrac{3}{2}\langle\sigma^2\rangle),$$

where M is the total mass. Introducing the calculated values of $\langle V_r^2\rangle$ and $\langle\sigma^2\rangle$, and the value of M derived from the model, one obtains

$$2T' = 2.49 \times 10^{50}\, r^2 \text{ ergs},$$

with r expressed in kpc.

The gravitational term is split into two parts, one giving the contribution of self-gravity and the other of the galactic gravitational field. The first of these has been calculated from the simplified Gaussian model, giving

$$W_1 = -8.59 \times 10^{47}\, r^3 \text{ ergs}.$$

The galactic contribution depends on the galactic gravitational field at the position of the cloud and the structure of the cloud. In case the object is located near the galactic centre the term may become comparable with the kinetic-energy term, and it can even become negative, the galactic field having a confining tendency, though it is likely that in the course of time the net effect of the galactic field will be disruptive. In view of the various unknown parameters entering into this problem I do not give any result beyond the statement that in the central region of the Galaxy the term may be important.

4.1. *A fragment of a supernova shell or of a past "superexplosion"*

As the total mass of the feature is $3.8 \times 10^4\ r^2 M_\odot$, the total expansion momentum should be $3.8 \times 10^4\ r^2 V_{exp}\ M_\odot$. If one admits as upper limit to the expansion momentum the value given by MINKOWSKI (1959) for a type II supernova, i.e., $7.5 \times 10^3\ M_\odot$ km/sec, and if one supposes that the feature observed at the velocity of +50 km/sec contains a fraction k of the entire shell, and that the present expansion velocity is 50 km/sec, then the equation of conservation of momentum gives $7.5 \times 10^3\ k = 3.8 \times 10^4 \times 50\ r^2$, and therefore, $r = 6 \times 10^{-2}\ k^{\frac{1}{2}}$ kpc.

If the feature observed is a fragment of an expanding supernova shell, the constancy of the velocity over the whole feature shows that it can represent only a relatively small fraction of the entire shell and k could certainly not be larger than 1/4, and would probably be considerably smaller. With $k = 1/4$ the maximum admissible distance becomes 30 pc. At such a small distance there would be likely to be optical evidence of the supernova shell. Both the short distance itself and the fact that no evidence of optical emission has been observed make the hypothesis of a fragment of a supernova shell somewhat implausible. The total hydrogen mass in the feature would, however, be of the order expected from a supernova shell.

We may also consider the possibility that the cloud is the result of a "superexplosion" which took place at a distance of 1 or 2 kpc from the Sun, at a location where the effect of differential rotation is still small. As was pointed out in section 2, the feature appears to be located in a region in which there is a deficiency of hydrogen at low velocities, as compared with the immediate surroundings. This could perhaps be explained by assuming that an explosion has occurred which has pushed away the matter connected with the ordinary galactic structure.

4.2. *An extragalactic object*

Table 3 gives a comparison between the two Magellanic Clouds and the feature. The distance of the feature has been derived from the virial theorem, assuming that equilibrium has been reached in the cloud, and attributing to it a total mass, M_t, of five times its hydrogen mass. There is good agreement between the characteristics of the three objects. Furthermore, the velocity with respect to the galactic centre, projected on the line of sight, is very small, so that the main argument proposed by Prata against an extragalactic explanation in the case of the cloud studied by him does not hold here.

TABLE 3

Comparison of the feature with the Magellanic Clouds

	LMC*	SMC**	Feature
r (kpc)	46	60	56
M_H ($M_\odot$)	3.8×10^8	5×10^8	10^8
M_t ($M_\odot$)	7.4×10^9	1.5×10^9	5×10^8
radius (kpc)	5	1.5	3

* R. X. MCGEE, 1965, *Mount Stromlo Symp. on the Magellanic Clouds* 34

** J. V. HINDMAN, 1967, *Australian J. Phys.* **20** 147

4.3. *A feature situated near the galactic centre*

In this case we might suppose that we observe matter ejected from the galactic nucleus, which is perhaps falling back into the galactic disk. This is based on the assumption that the line passing through the intensity maxima as shown in figure 6 is the trace on the plane of the sky of matter which has been ejected continuously from the nucleus. The characteristic expansion time of the feature computed from the kinetic term in

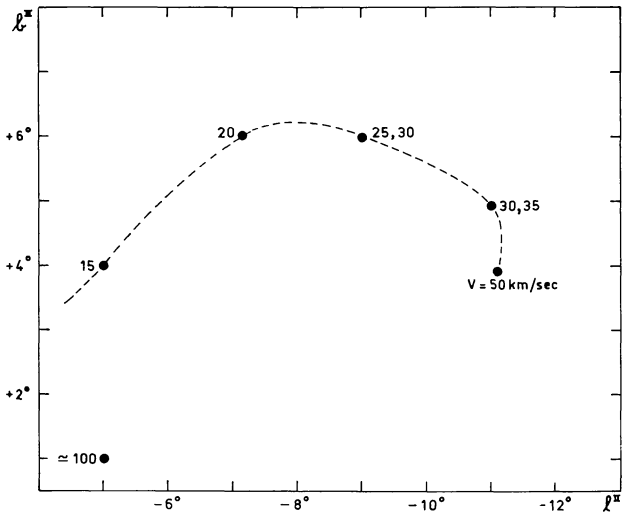

Figure 6. Representative positions of the maximum brightness temperature as a function of velocity. No account was taken of the maxima due to the normal galactic structure. A smooth curve has been drawn through the points.

the virial theorem is about 10^7 years, and is long enough to have permitted matter ejected from the centre to reach a distance greater than 2 kpc, with a velocity of ejection of 200 km/sec. It is interesting at this point to consider ROUGOOR's (1964) investigation concerning a high positive velocity feature at low positive latitudes and negative longitudes, which he assumes to be an inner expanding arm. Both phenomena have perhaps the same origin, and might possibly be explained by the same model.

4.4. *An ordinary high-velocity cloud*

Table 2 gives the physical parameters of the feature at various distances from the Sun. At a distance of the order of 1 kpc the density becomes of the same order as the density of the surrounding galactic hydrogen. The corresponding radius is about 50 pc.

If the distance is about 1 kpc the feature would be similar to other high- or intermediate-velocity concentrations, except for the radial velocity, which is in most cases negative, although a few concentrations with positive velocity are known, but with smaller densities than this feature. It is possible that more concentrations similar to this one would be found at low longitudes and at latitudes below 15°, a region which has not been fully investigated. Such concentrations might have properties different from the high-velocity clouds thus far investigated. To conclude, no argument can be found at this point against or in favour of this hypothesis. A search in this direction for interstellar absorption lines would perhaps provide the answer.

4.5. *A distant arm of the Galaxy*

As noted above, it is possible to follow, on Kerr's contour diagrams, a feature at high positive velocity (from 45 to 60 km/sec) running from $l^{II} = -13°$ to $l^{II} = -19°$ and perhaps further (the available observations stop at this longitude). In order to investigate if the feature described in the present paper is connected with Kerr's concentration, I plotted on a diagram in l^{II} and V_r, following HABING's (1966) method, the run of peak velocities. These velocities have been averaged for latitudes between 2° and 6°, using Dwingeloo material, while more approximate, but still reliable, values have been deduced from combined Dwingeloo-Australian observations at $b^{II} = 1°$ and 2°. This procedure has been chosen in order to preserve the evidence of two peaks appearing in the Dwingeloo observations, i.e., at about +30 and +50 km/sec, as quoted in section 3. The result is shown in figure 7.

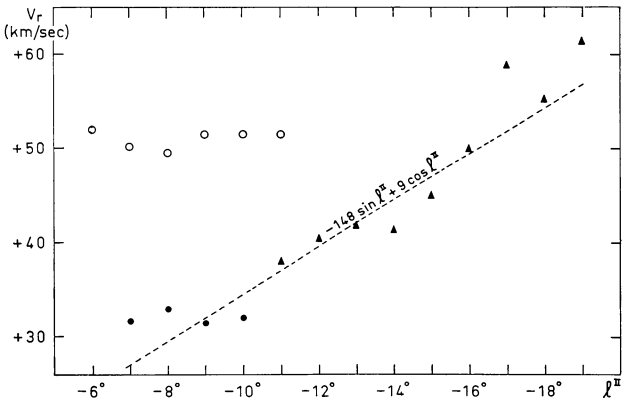

Figure 7. Peak velocities arising from the features studied here. Open circles are the 50-km/sec feature, filled circles the 30-km/sec peak and triangles the high-velocity concentration appearing in Kerr's contour diagrams.

The following remarks can be made: 1) The 30-km/sec feature seems to be the natural prolongation of Kerr's feature. Furthermore, peak intensities are of the same order in both cases (from 15 to 25 °K), and higher than the maximum intensity at 50 km/sec. 2) Velocities for the 30-km/sec peak increase with decreasing longitude. 3) The 50-km/sec peak has a nearly constant velocity. It seems reasonable to assume that the feature appearing in Kerr's diagrams and the 30-km/sec peak represent a very distant arm. The representative points in figure 7 fit rather well with the law

$$V = (148 \sin l^{II} + 9 \cos l^{II}) \text{ km/sec},$$

which implies a distance of about 19 kpc from the galactic centre* and an expansion velocity of 9 km/sec. This must be considered as an estimate; a more reliable fit would require many more points. However, this is good enough for the present purpose, which is to see if a relation between the 50-km/sec feature and this assumed very distant arm is possible. The fact that the velocity of the 50-km/sec gas does not change with longitude implies a much higher velocity of expansion than 9 km/sec, if it should be located at a similar distance as the arm. On the other hand, if a smaller expansion velocity is assumed, say 20 km/sec, the dis-

* In estimating this distance I have used the rotation curve given by SCHMIDT (1965).

tance of the feature from the centre increases to about 30 kpc or more. In conclusion, if there is an outer arm, any connection between it and the feature discussed in the present paper seems unlikely; the hypothesis that the 50-km/sec gas represents another outer arm is equally implausible.

Acknowledgements

I would like to acknowledge a grant from the Belgian National Foundation for Scientific Research (F.N.R.S.) The same organization contributed financially to my stay in the Netherlands. I wish to express my gratitude to Professor Dr. J. H. Oort, for his hospitality at the Leiden Observatory and for his helpful guidance and criticism. I am also very much indebted to W. W. Shane who gave me many useful suggestions and encouragement, and kindly corrected the manuscript. My thanks are due also to Dr. F. J. Kerr for permitting the use of his observations. The observations were financially supported by the Netherlands Organization for the Advancement of Pure Research (Z.W.O.). The reduction was performed on the Electrologica X1 computer of the University at Leiden, and further calculations were made partly with the aid of the IBM 7040 computer of the University at Liège.

References

H. J. Habing, 1966, *Bull. Astr. Inst. Netherlands* **18** 323
R. Minkowski, 1959, *Symp. I.A.U.* **9** 315
C. A. Muller and G. Westerhout, 1957, *Bull. Astr. Inst. Netherlands* **13** 151
C. A. Muller, E. Raimond, U. J. Schwarz and C. R. Tolbert, 1966, *Bull. Astr. Inst. Netherlands Suppl.* **1** 213
S. W. Prata, 1964, *Bull. Astr. Inst. Netherlands* **17** 511
E. Raimond, 1966, *Bull. Astr. Inst. Netherlands Suppl.* **1** 33
G. W. Rougoor, 1964, *Bull. Astr. Inst. Netherlands* **17** 381
M. Schmidt, 1965, *Galactic Structure*, ed. A. Blaauw and M. Schmidt (Univ. of Chicago Press, Chicago) chapter 22

Figure 2 (pp. 371–373). The reduced and averaged line profiles. The secondary peak at +50 km/sec is the subject of this investigation.